LIQUID CRYSTALS
2020, VOL. 47, NO. 5, 715–722
https://doi.org/10.1080/02678292.2019.1673842

Taylor & Francis
Taylor & Francis Group

Check for updates

Spatially and electrically tunable random lasing based on a polymer-stabilised blue phase liquid crystal-wedged cell

Ruochen Liao, Xiyun Zhan, Xiaowan Xu, Yanjun Liu, Fei Wang and Dan Luo

Department of Electrical and Electronic Engineering, Southern University of Science and Technology, Shenzhen, Guangdong, China

ABSTRACT

We demonstrate a spatially and electrically tunable random lasing based on polymer-stabilized blue phase liquid crystal (PS-BPLC)-wedged cell. The spatially tunable random lasers can be obtained from the laser dye-doped PS-BPLC-wedged cell through changing the pump positions, where the emission wavelength of the random laser can be tuned due to the thickness gradient of the wedged cell, which affects the scattering mean free path. Additionally, applying different electric fields can also tune the laser emission wavelength. The changing of refractive index due to the Kerr effect leads to a change in the scattering mean free path, resulting in shift of lasing wavelength. This PS-BPLC-wedged cell device has a great potential in applications of speckle-free imaging, document coding, biomedicine and other photonic devices.

ARTICLE HISTORY
Received 14 April 2019
Accepted 25 September 2019

KEYWORDS
Liquid crystal; blue phase; random lasing; polymer; tunable

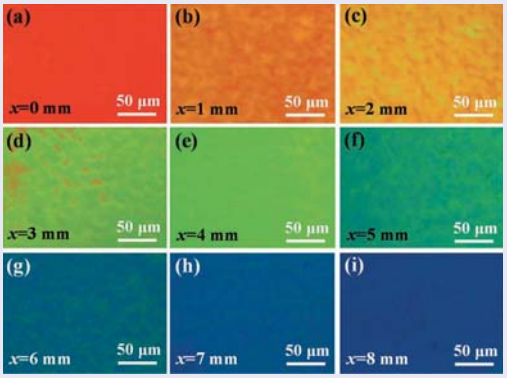

POM images of gradient-pitched PS-BPLC-wedged cell at different positions of (a) x=0 mm; (b) x=1 mm; (c) x=2 mm; (d) x=3 mm; (e) x=4 mm; (f) x=5 mm; (g) x=6 mm; (h) x=7 mm; (i) x=8 mm. The scale bar is 50 μm.

Introduction

Random laser has received great attention in recent years due to its unique lasing mechanisms and special characteristics like low spatial coherence, multiple laser wavelengths and omnidirectional emission [1,2]. The generation of a random laser does not require a reflector cavity compared with the traditional laser, the optical feedback of a random laser is obtained by multiple scattering in a gain medium [3,4]. Therefore, recurrent multiple scattering in the diffusion medium is crucial to the generation of random lasers. Many materials, such as ZnO, $CuSO_4$ and Au nanoparticles, semiconductor powder, biological structures and liquid crystals can be used to fabricate random lasers [5–9]. Attributed to the generation mechanism, the random laser has many potential applications including speckle-free imaging, document coding, biomedicine and medical diagnostics [3,9,10].

Liquid crystal (LC), which possesses large index birefringence and light-scattering ability, is an ideal candidate to produce random laser. Under external fields such as electric field, magnetic field, optical irradiation or environmental temperature, the LC molecules will reorient or disorder, which will influence the emission of random laser [11,12]. A series of studies have been reported to obtain random lasing in different LC materials, including nematic, cholesteric, smectic and sphere phase LCs [12–15]. Blue phase liquid crystal (BPLC), an intermediate stable phase between the chiral nematic phase and the isotropic phase, usually with a narrow temperature range about 0.5–2°C [16], shows great

CONTACT Dan Luo luod@sustech.edu.cn
© 2019 Informa UK Limited, trading as Taylor & Francis Group

potential in generating random laser. By photo-polymerisation, the BPLC can be stabilised and its stable temperature can be largely extended, leading to a broader range of display and photonic applications [17]. In the three-dimensional (3D) self-assembled photonic-bandgap structures of BPLC, lasing can be generated [2], not only band-edge lasing due to its periodic 3D structure, but also random lasing due to the light scattering effect in the discontinuous platelets boundaries in BP or index mismatch between polymer and LC in polymer-stabilized blue phase liquid crystal (PS-BPLC) [11].

Several studies about BPLC random laser have been demonstrated. Chen et al. reported random lasing actions and emission characteristics in BPLC and PS-BPLC, respectively [11]. They have found that the cooling rate is related to platelet size, thus affects the lasing randomness. Wang et al. observed the bichromatic coherent random lasing actions from the dye-doped PS-BPLC. The relative intensity between the two peak groups could be controlled by the polarisation of the pump light [18]. In addition, the random laser has also been proved to be electrically or thermally adjusted [19]. However, current works have only reported the tuning of lasing intensity, the tuning of lasing wavelength of BPLC random laser is far from fully investigated. As for the tuning of lasing wavelength, many studies related to dye-doped cholesteric liquid crystal (DDCLC) were reported by adjusting the external factors like temperature, electric field, pumping energy or positions [20–22].

In this study, we demonstrate a spatially and electrically tunable random laser based on polymer-stabilized blue phase liquid crystal (PS-BPLC) wedged cell. The fabrication process of the PS-BPLC-wedged cell is based on the blue-phase templated fabrication proposed by Castles et al. [23]. The polymer network film can retain BP through the wash-out process, leading to great tunability of the refilling materials and the film. By using the wedged cell, a non-uniform wedged polymer network structure can be obtained, which will affect the pitch length of BP at different positions of the cell. The random laser based on PS-BPLC-wedged cell possesses low cost, small volume, high stability and variability. The emission wavelength of the random laser can be tuned by changing the pump positions and electric field, which provides it with great potential on speckle-free imaging, document coding, medical diagnostic and other photonic devices.

Experiments

In our experiment, the LC/monomer composite consisted of 82.05 wt.% nematic LC HTG135200, 2.95 wt.% chiral dopant R5011, 11 wt.% monomer 1,4-Bis-[4-(3-acryloyloxypropyloxy) benzoyloxy]-2-methylbenzen (RM257), 3 wt.% monomer trimethylolpropane triacrylate (TMPTA) (all from HCCH), and 1 wt.% photoinitiator Darocur1173 (from Sigma-Aldrich, Germany). The material showed the following phase sequence: ISO (85°C)-BPI (71°C)-N*. A LC cell that was assembled by two indium-tin-oxide (ITO)-coated glass substrates with anti-parallel rubbing was used to form PS-BPLC film. The original thickness of LC cell was 10 μm, where two layers of spacers with diameter of 10 μm were applied to control the gap of LC cell (as shown in Figure 1).

To fabricate the PS-BPLC-wedged cell, the prepared LC/monomer composite was firstly heated up to an isotropic phase (85°C) through a hot stage (HCS402, INSTEC, USA) and then slowly cooled down to 71°Cat rate of 0.1°C/min. Next, the sample was exposed in ultraviolet (UV) light (365 nm) with an intensity of 20 mW/cm^2 for 15 min, resulting in a uniform PS-BPLC film in BP I phase. After that, the sample was soaked in toluene for 12 h to wash out LCs and unpolymerised monomers (Step I), leaving a polymer network with 3D nanostructure. Then, the LC cell was opened and one layer of spacer with 10 μm diameter was replaced by a layer of spacer with 5 μm diameter (mixed with glue), leading to a wedged structure of polymer network. Finally, laser dye 4-(dicyanomethylene)-2-methyl-6-(4-dimethylaminostyryl)-4H-pyran (DCM) doped nematic LC (HTG135200) was refilled into the wedged polymer network, resulting in a PS-BPLC-wedged cell. The mixture refilled into the gradient-pitched PS-BPLC-wedged cell consists of 1 wt.% DCM and 99 wt.% HTG135200. After the mixture was refilled into the cell, the sample was heated up to 60°C. The thickness of wedged cell was changed from 5 to 10 μm, and the pitch of PS-BPLC film was depressed due to external press for region with thickness less than the 10 μm (original thickness). The length of the PS-BPLC-wedged cell along x-axis (as shown in Figure 1) was around 10 mm. At different lines in x-y plane, such as from x = 0 mm to x = 10 mm, the PS-BPLC-wedged cell possessed different pitch and the reflection colour changed from red to blue.

Figure 2 shows the optical images of the gradient-pitched PS-BPLC-wedged cell measured at different positions under orthogonal polarised optical microscope (POM) (Nikon, Ci-POL). Figure 2(a-i) illustrate the continuous change of colour from red to blue of the gradient-pitched PS-BPLC-wedged cell corresponding to position of x = 0, 1, 2, 3, 4, 5, 6, 7 and 8 mm, respectively. The corresponding cell thicknesses at the specific lateral positions are 10, 9.5, 9, 8.5, 8, 7.5, 7, 6.5

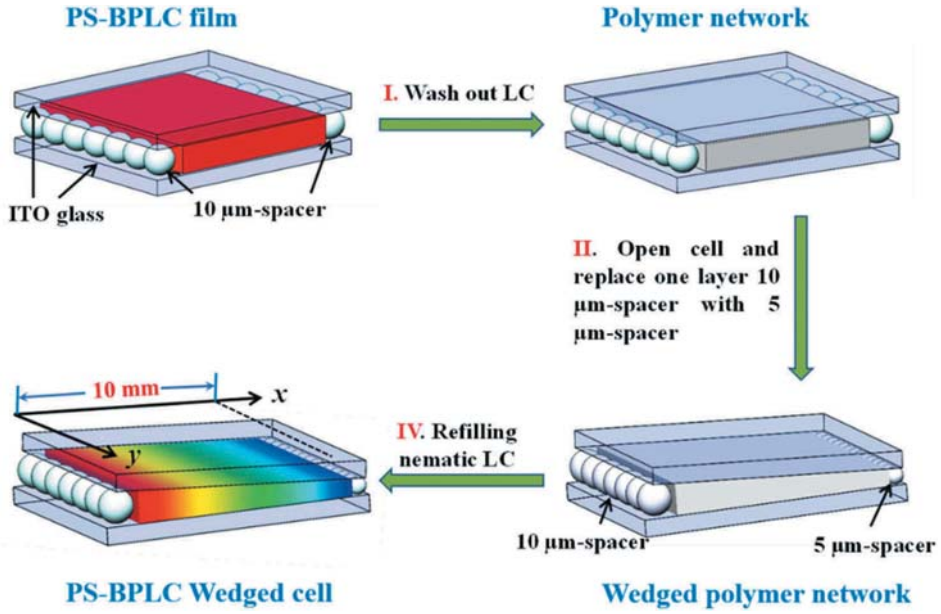

Figure 1. (Colour online) Schematic of fabrication process of polymer-stabilized blue phase liquid crystal-wedged cell.

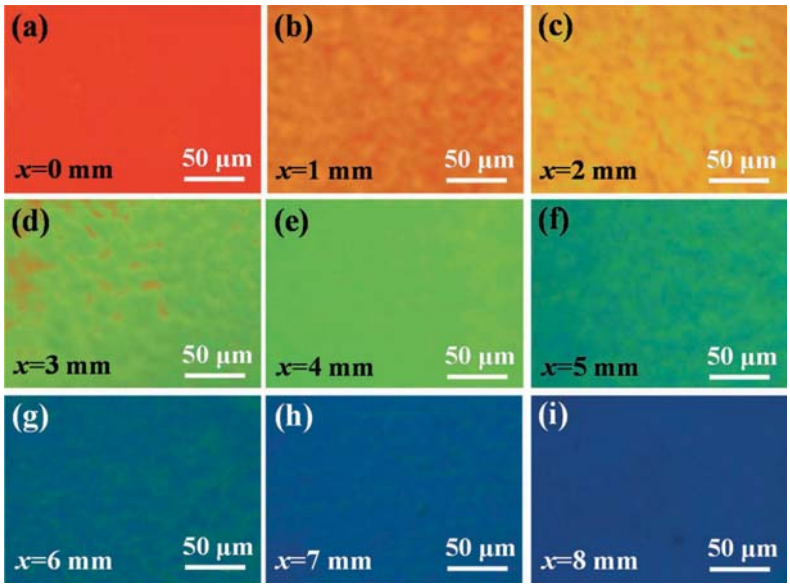

Figure 2. (Colour online) POM images of gradient-pitched PS-BPLC-wedged cell at different positions of (a) $x = 0$ mm; (b) $x = 1$ mm; (c) $x = 2$ mm; (d) $x = 3$ mm; (e) $x = 4$ mm; (f) $x = 5$ mm; (g) $x = 6$ mm; (h) $x = 7$ mm; (i) $x = 8$ mm. The scale bar is 50 μm.

and 6 μm, respectively. The wedged cell forms a continuous varying gradient of boundary force, resulting in a gradient lattice structure of BP I at different regions, thus the BP micro-platelets in different regions can reflect the incident light selectively. As the thickness of the wedged cell decreases, the reflection colour gradually changes from red to blue, leading to a rainbow-like reflection pattern. The colour is from the selective reflection due to the chiral structure.

Figure 3 shows the reflection spectra of the PS-BPLC-wedged cell measured at different lateral positions of $x = 0$, 2, 4, 6 and $x = 8$ mm, respectively. The spectral measurements were performed at room temperature 25°C. The cell thickness decreases with the increase of x from $x = 0$ to $x = 8$ mm, which leads to a 124 nm blue-shift of photonic band gap in reflection spectrum from red (621 nm) to blue (497 nm). In PS-BPLC, the reflection is due to the selective Bragg reflection based on 3D

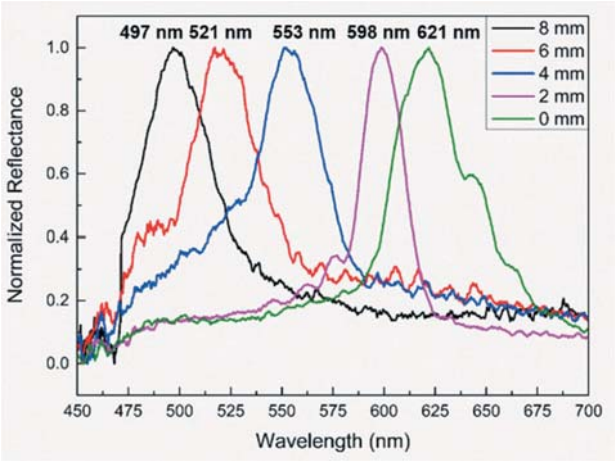

Figure 3. (Colour online) Reflection spectra of the PS-BPLC-wedged cell measured at different position of x = 0, 2, 4, 6 and 8 mm, respectively. 124 nm peak shift of reflection spectrum is observed when the position changes from x = 0 to x = 8 mm.

periodic structure formed by double-twisted self-assembled LC molecules. The reflection wavelength of the PS-BPLC for normal incidence can be shown as $\lambda = 2na/\sqrt{h^2 + k^2 + l^2}$, where n and a denote the effective refractive index and lattice constant, respectively; h, k and l are the Miller indices of a crystal plane [24]. Here, the n can be expressed as $n = (n_e + 2n_o)/3$, where n_e and n_o are the extraordinary and ordinary refractive indices of the LC molecules. The lattice constant a depends on the pitch length of the BP I in PS-BPLC cell. Before step α, the central wavelength in the reflection band of the uniform BP I polymer network with (0, 1, 1) plane was 630 nm, which was being adjusted by the concentration of chiral dopant. Under the external force formed by the inclined glass, the polymer network structure was depressed, leading to the change of pitch length at different positions along x-axis. Then the refilled LC and laser dye will fill in the double-twisted cylinder structure because of the specific alignment effect of polymer network. BP I with different pitch and reflection wavelength reappeared.

The experimental setup for lasing generation form PS-BPLC-wedged cell is shown in Figure 4. A Q-switched Nd:YAG laser with centre wavelength of 532 nm, pulse duration of 10 ns and repetition rate of 10 Hz was used as the pump source. The incident linear polarised laser beam was divided into two beams by a beam splitter after passing through a 532 nm green light filter which is a spatial filter used to improve the laser beam quality with erasing the spatial high frequency, and an attenuator which was used to adjust the intensity of the pump laser. One divided beam was collected by a power detector to monitor the power of pump laser, and another beam (transmitted) was focused by a cylindrical lens to a strip and impinged on the sample wedged cell. The pump area is about 0.5 mm^2. The energy density is about 260 μJ/mm^2 per pulse. Inset shows the photo of sample, where the PS-BPLC-wedged cell demonstrated from red to violet colours at different positions with the increase of x. It was noticed that the colour changed uniformly at the whole cell from one side to the other along x-axis, which was due to the fabrication error in wedged cell fabrication procedure. Therefore, to make sure the uniformly change of wedged cell, a small region (rectangle in white dash line) was selected for lasing generation. The focused pump laser beam in form of strip was adjusted along the line of $x = l$ (l = 0 to 10 mm) in x-y plane. The omni directional output laser was collected along the direction of – y as shown by the red arrow where the lasing can be guided and the intensity is a little higher.

Results and discussions

Figure 5 shows the laser spectrum generated at different lateral positions of x = 0, 2, 4, 6 and 8 mm, respectively, at room temperature. A typical random lasing can be

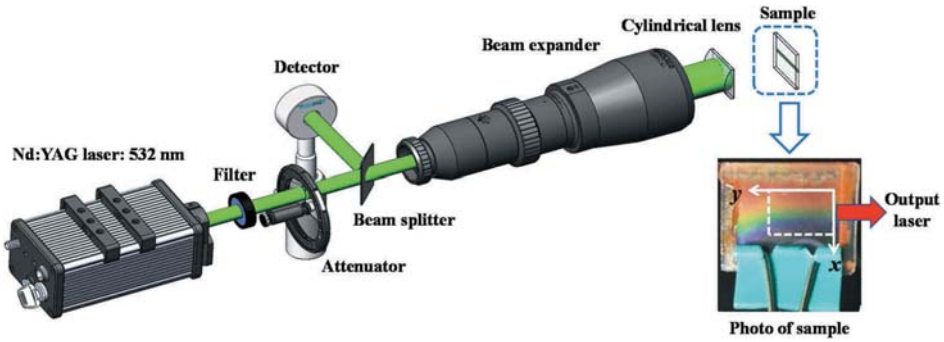

Figure 4. (Colour online) Schematic of experimental setup for lasing generation.

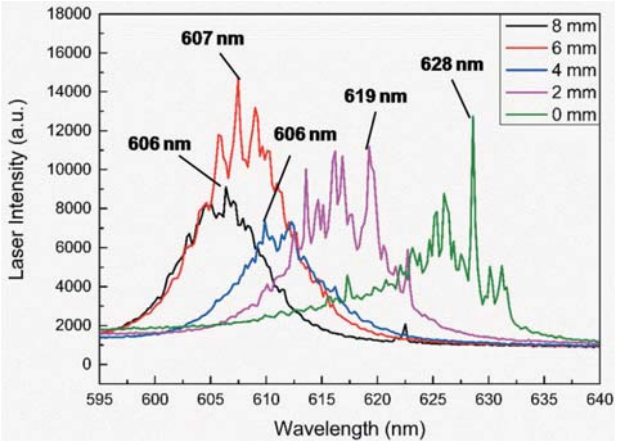

Figure 5. (Colour online) (a) Lasing spectra of the gradient-pitched PS-BPLC-wedged cell generated from position of x = 0, 2, 4, 6 and 8 mm, respectively.

observed with multi-peaks. The maximal lasing peaks are marked in Figure 5 as well. With the changes of pump position from x = 0 mm to x = 8 mm, the peak wavelength of the emitted lasing is gradually blue-shift and the spatially tunability of lasing wavelength range is realised from 606 to 628 nm, with 22 nm tunable range.

The combined reflection and emission spectra are shown in Figure 6(a-e) for position of x = 0, 2, 4, 6 and 8 mm. It is noticed that the peak wavelength of the lasing spectrum is not overlapped with the corresponding band-edge of the reflection spectrum, especially on the thin side of the PS-BPLC cell. In addition, the output lasing is not polarisation sensitively, while the band-edge laser will usually emit circularly polarised light. This phenomenon proves that the laser emission observed here is not the band-edge type lasing but random lasing.

The mechanism of the formation of a random laser is multiple scattering in the medium [11]. The multiple scattering not only comes from the randomly distributed BP platelets and the discontinuous boundaries, but also the index mismatch between the polymer and the refilled LC molecules. The light waves that are emitted from the laser dye travel along the BP platelets, leading

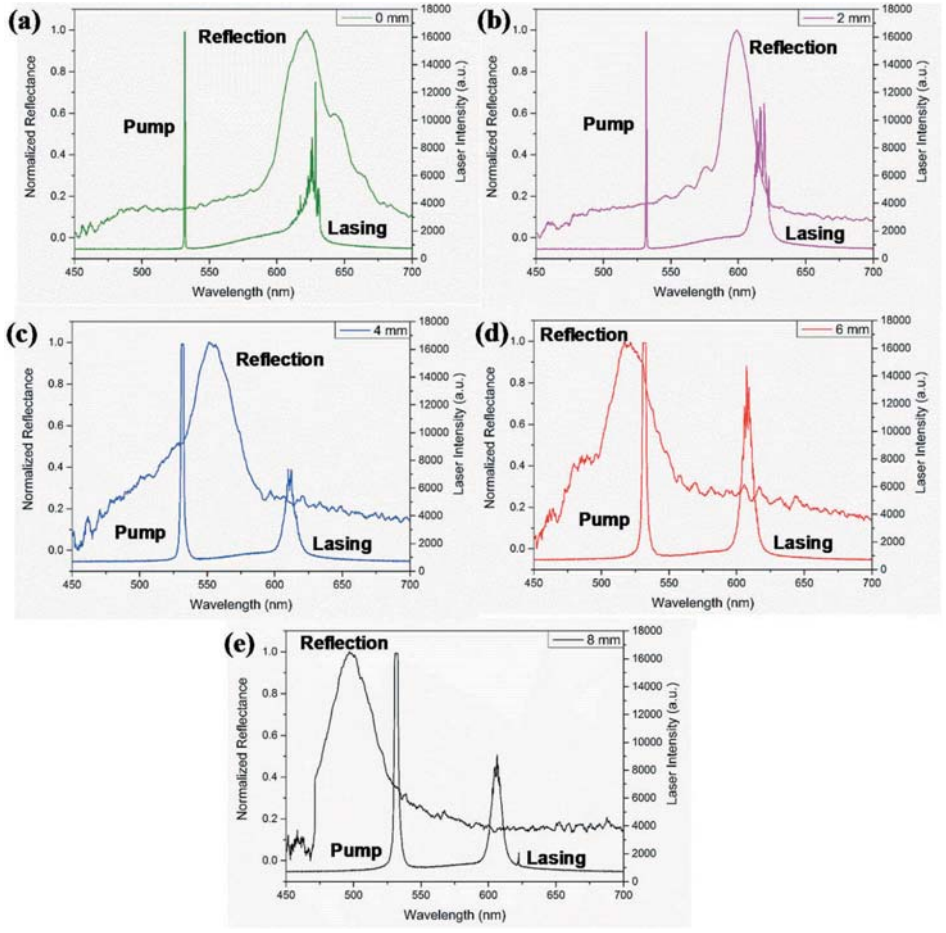

Figure 6. (Colour online) Combined reflection and emission spectra at position of (a) x = 0 mm, (b) x = 2 mm, (c) x = 4 mm, (d) x = 6 mm, and (e) x = 8 mm, respectively.

to multiple scattering. Then part of the light waves goes back to the beginning position. The light experiences both loss and amplification along the closed-loop path during scattering. In that case, random lasing appears when gain is higher than loss. The scattering mean free path is a key factor for random lasers emission and influences the wavelength of the emission laser. In a scattering system, the random lasing wavelength is closely related to the scattering mean free path l_s [25]. Hu et al. demonstrated that the random lasing wavelength with short l_s exhibited blue-shift effect compared to that with long l_s in the tunable random polymer fibre laser [26]. Herein, scattering occurs at the boundaries between BP platelets, and between general defects in the BPLC structure. As the PS-BPLC material inside the cell is compressed into thinner regions of the wedged cell, the spaces between the scattering centres will decrease. Therefore, the emitted light has a shorter dwelling time in the thin region than the thick region, which leads to the reduction of the value of the scattering mean free path l_s and the blue-shifted laser emission.

We also analysed the threshold behaviour of the lasing at different positions of the PS-BPLC-wedged cell. As shown in Figure 7, at the positions of x = 0, 2, 4, 6 and 8 mm, the pump energies are 50, 80, 95, 105 and 130 μJ/pulse, respectively. With the decrease of the cell thickness, the threshold will increase.

The random laser emission from the gradient-pitched PS-BPLC-wedged cell can be also controlled by applying external alternating current (AC) electric field. Figure 8 plots the laser spectra of the PS-BPLC–wedged cell under different applied voltages at the pump position of x = 1 mm. The peak wave length of lasing red-shifts from 617 nm to 634 nm while the applied voltage increases from 0 V to 150 V. The redshift of lasing peak turns to be saturated when applied voltage reaches 150 V. Meanwhile, the lasing intensity decreased obviously under the increase of electric field.

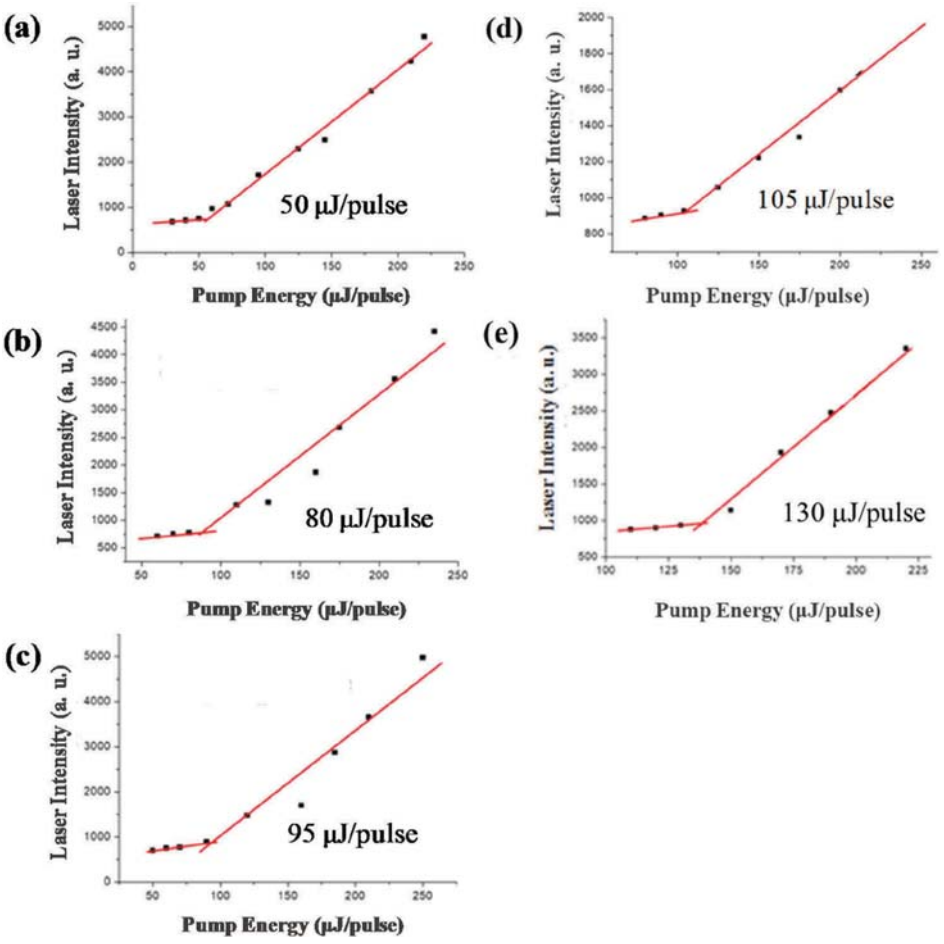

Figure 7. (Colour online) Laser intensity of the PS-BPLC laser at a function of pump energy at different positions of the wedged cell. (a) x = 0 mm, (b) x = 2 mm, (c) x = 4 mm, (d) x = 6 mm, and (e) x = 8 mm.

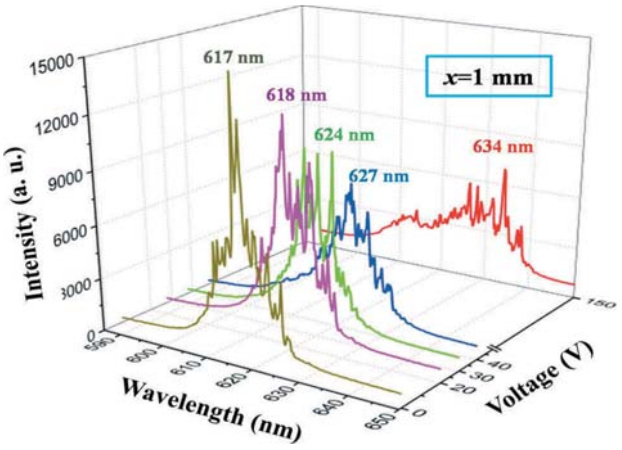

Figure 8. (Colour online) Lasing spectra of the gradient-pitched PS-BPLC-wedged cell pumped at position of x = 1 mm under different applied voltage.

When the applied voltage increases, the LC molecules will reorient and follow the direction of the electric field, leading to the decrease of the multiple scattering and the birefringence of blue phase will be induced. In the high field region, the induced birefringence can be described by the following mathematical expression [27]:

$$\Delta n_{ind} = \Delta n_{\mathrm{sat}}\left\{1 - exp\left[-\left(E/E_S\right)^2\right]\right\} \qquad (1)$$

where Δn_{sat} stands for the saturated induced birefringence and E_S represents the saturation field. Decreasing the medium's refractive index n will increase the value of l_s, resulting in a red-shift effect of the emitted lasing. When the electric field is added on the PS-BPLC cell, it reorients LC molecules to align along the z direction that is perpendicular to the substrate. However, the direction of the emitted lasing is along y direction, which is perpendicular to the direction of the electric field. Therefore, when the electric field is applied, the effect index of LC in x-y plane reduces. The medium's average refractive index n is reduced due to Kerr effect and saturated under a high electric field, resulting in the increase of l_s and a red-shift of the emitted random lasing as shown in Figure 7.

Conclusion

In summary, this work demonstrates a spatially and electrically tunable random laser based on PS-BPLC-wedged cell. A gradient of boundary force caused by the wedged cell leads to a gradient lattice in the BP crystal structure, which causes a continuously shifting photonic bandgap. The random lasers can be obtained from the dye-doped PS-BPLC-wedged cell. By changing the pump positions, the emission wavelength of the random laser can be tuned due to the thickness gradient of the wedged cell, which affects the scattering mean free path. Additionally, applying different electric fields can also tune the emission wavelength. The changing of refractive index due to the Kerr effect leads to a change in the scattering mean free path, resulting in shift of lasing wavelength. Such a PS-BPLC-wedged cell device has a great potential in applications of speckle-free imaging, document coding, biomedicine and other photonic devices.

Disclosure statement

No potential conflict of interest was reported by the authors.

Funding

This work is supported by National Natural Science Foundation of China (NSFC) [61875081], Shenzhen Science and Technology Innovation Commission [JCYJ20180305180700747, and JCYJ20160226192528793].

References

[1] Coles H, Morris S. Liquid-crystal lasers. Nat Photon. 2010;4(10):676–685.
[2] Cao W, Muñoz A, Palffy-Muhoray P, et al. Lasing in a three-dimensional photonic crystal of the liquid crystal blue phase II. Nat Mater. 2002;1(2):111–113.
[3] Wiersma DS. The physics and applications of random lasers. Nat Phys. 2008;4(5):359–367.
[4] Lawandy NM, Balachandran RM, Gomes ASL, et al. Laser action in strongly scattering media. Nature. 1994;368(6470):436–438.
[5] Yu SF, Yuen C, Lau SP, et al. Random laser action in ZnO nanorod arrays embedded in ZnO epilayers. Appl Phys Lett. 2004;84(17):3241–3243.
[6] Shang Z, Tao Z, Deng L. Random lasing assisted by $CuSO_4$ and Au nanoparticles in random gain systems. Opt Mater Express. 2017;7(6):1848–1857.
[7] Cao H, Zhao YG, Ho ST, et al. Random laser action in semiconductor powder. Phys Rev Lett. 1999;82(11):2278–2281.
[8] Huang DF, Xu M, Liu XY, et al. Low threshold random lasing actions in natural biological membranes. Laser Phys Lett. 2016;13(6):065603.
[9] Polson RC, Vardeny ZV. Random lasing in human tissues. Appl Phys Lett. 2004;85(7):1289–1291.
[10] Redding B, Choma MA, Cao H. Speckle-free laser imaging using random laser illumination. Nat Photon. 2012;6(6):355–359.
[11] Chen CW, Jau HC, Wang CT, et al. Random lasing in blue phase liquid crystals. Opt Express. 2012;20(21):23978–23984.
[12] Zhu JL, Li WH, Sun Y, et al. Random laser emission in a sphere-phase liquid crystal. Appl Phys Lett. 2015;106:191903.

[13] Sznitko L, Kaliciak K, Adamow A, et al. A random laser made of nematic liquid crystal doped with a laser dye. Opt Mater. 2016;56:121–128.
[14] Morris SM, Gardiner DJ, Hands PJW, et al. Electrically switchable random to photonic band-edge laser emission in chiral nematic liquid crystals. Appl Phys Lett. 2012;100:071110.
[15] Morris SM, Ford AD, Pivnenko MN, et al. Electronic control of nonresonant random lasing from a dye-doped smectic A* liquid crystal scattering device. Appl Phys Lett. 2005;86:141103.
[16] Meiboom S, Sammon M. Structure of the blue phase of a cholesteric liquid crystal. Phys Rev Lett. 1980;44 (13):882–885.
[17] Kikuchi H, Yokota M, Hisakado Y, et al. Polymer-stabilized liquid crystal blue phases. Nat Mater. 2002;1 (1):64–68.
[18] Wang L, Wang M, Yang M, et al. Bichromatic coherent random lasing from dye-doped polymer stabilized blue phase liquid crystals controlled by pump light polarization. Chin Phys B. 2016;25 (9):094217.
[19] Lee CR, Lin SH, Guo JW, et al. Electrically and thermally controllable nanoparticle random laser in a well-aligned dye-doped liquid crystal cell. Opt Mater Express. 2015;5(6):1469–1481.
[20] Dadalyan T, Alaverdyan R, Nys I, et al. Tuning thelasing wavelength of dye-doped chiral nematicliquidcrystal by fluid flow. Liq Cryst. 2017;44(2):372–378.
[21] Dadalyan T, Ninoyan Z, Nys I, et al. Light-induced multi-wavelength lasing in dye-doped chiral nematic liquid crystals due to strong pumping illumination. Liq Cryst. 2018;45(9):1272–1278.
[22] Li Y, Du QG, Liu ZD, et al. Pump angle and position effects on laser emission from quasicrystal microcavity by nine-beam interference based on holographic polymer-dispersed liquid crystals. Liq Cryst. 2018;45 (3):415–420.
[23] Castles F, Day FV, Morri SM, et al. Blue-phase templated fabrication of three-dimensional nanostructures for photonic applications. Nat Mater. 2012;11(6):599–603.
[24] Heppke G, Kitzerow HS, Krumrey M. Angular dependence of blue phase selective reflection in the electric field. Mol Cryst Liq Cryst. 1987;150(1):265–276.
[25] Wu XH, Yamilov A, Noh H, et al. Random lasing in closely packed resonant scatterers. J Opt Soc Am B. 2004;21(1):159–167.
[26] Hu Z, Xia J, Liang Y, et al. Tunable random polymer fiber laser. Opt Express. 2017;25(15):18421–18430.
[27] Yan J, Li Y, Wu ST. High-efficiency and fast-response tunable phase grating using a blue phase liquid crystal. Opt Lett. 2011;36(8):1404–1406.